

This suggests that the electron transfer between superoxide and copper is not mediated by a water molecule near the copper ion. The activity profiles of the WT and of the three mutants at the 137 position are virtually identical, except for a small decrease in the high-pH pK_a of the profile of Ile-137. The first conclusion would be that the kinetic parameters are not much dependent on the nature of the residue at position 137, provided that the WT is the most active derivative. The affinity of N_3^- increases slightly from Ser-137 to WT and Ala-137. Then it is almost 50% larger for the Ile-137 derivative. The azide affinity follows the reverse order of the water $^1H T_1^{-1}$ values. It has been independently proposed that the affinity of O_2^- (and therefore K_M) changes in the same direction as N_3^- does in a series of mutants at position 143.²² Here, the overall changes are much smaller and not easily related to N_3^- affinity. In the previous series of mutants, the changes were proposed to originate mainly from electrostatic reasons, the mutated residue being a positively charged arginine. Here, the factors governing activity and anion affinity may not be the same, and in many cases they induce smaller effects.

The variation in the high-pH pK_a of the activity profile in the case of Ile-137 is likely due not to structural effects but only to change in hydrophobicity of the cavity. The small inflection at about pH 6-7 is also due to groups yet undefined; interestingly, it is present also in the mutants without Glu-132 and Glu-133, which are at the opening of the cavity.¹³ It may be due to a different group far from the active cavity. Therefore the pH dependence of the activity around neutrality is quite complex.

Acknowledgment. Thanks are expressed to Professor B. H. J. Bielski (Brookhaven National Laboratory) and to Dr. G. T. Mullenbach (Chiron Corp.) for helpful suggestions. This work has been performed with a financial contribution from Chiron Corp. The pulse radiolysis studies were supported under NIH Grant RO1 GM23656-10 and carried out at Brookhaven National Laboratory.

Registry No. Ser, 56-45-1; Ala, 56-41-7; Ile, 73-32-5; Thr, 72-19-5; Cu, 7440-50-8; N_3 , 14343-69-2; superoxide dismutase, 9054-89-1.

Contribution from the Department of Chemistry,
Louisiana State University, Baton Rouge, Louisiana 70803-1804

Intramolecular Binding of Nitrogen Bases to a Cofacial Binuclear Copper(II) Complex†

Andrew W. Maverick,* Michael L. Ivie, John H. Waggenspack, and Frank R. Fronczek

Received May 2, 1989

Coordination of pyrazines and pyridines to the cofacial binuclear complex $Cu_2(NBA)_2$ ($NBAH_2 = 3,3'-[2,7-naphthalenediylbis(methylene)]bis(2,4-pentanedione)$) has been studied by structural and spectroscopic methods. Pyrazines bind more strongly than the corresponding pyridines, suggesting intramolecular, or endo, coordination, which X-ray analysis of the adduct with 2,5-dimethylpyrazine (2,5-Me₂pyz) confirms: $Cu_2(NBA)_2(\mu-2,5-Me_2pyz) \cdot 4CH_2Cl_2$, monoclinic, space group $C2/m$ (No. 12); $a = 22.941$ (6), $b = 22.432$ (4), $c = 11.677$ (2) Å; $\beta = 97.32$ (2)°; $V = 5960$ (4) Å³; $Z = 4$; $R = 0.096$, $R_w = 0.093$ for 372 parameters and 3358 reflections with $I > 1\sigma(I)$. The structure contains two independent $Cu_2(NBA)_2(\mu-2,5-Me_2pyz)$ molecules ($Cu \cdots Cu = 7.596$ (2), 7.559 (2) Å), each with a disordered 2,5-Me₂pyz moiety and overall $2/m$ (C_{2h}) symmetry. Equilibrium constants for binding of substituted pyrazines to $Cu_2(NBA)_2$ range from ca. $0.2 M^{-1}$ (2,3-diethylpyrazine) to $93 M^{-1}$ (2-aminopyrazine); binding constants for comparably substituted pyridines are significantly smaller in all cases. Hydrogen bonding between the NH_2 group of 2-aminopyrazine and the O atoms of the $Cu_2(NBA)_2$ host is probably responsible for its unusually large binding constant.

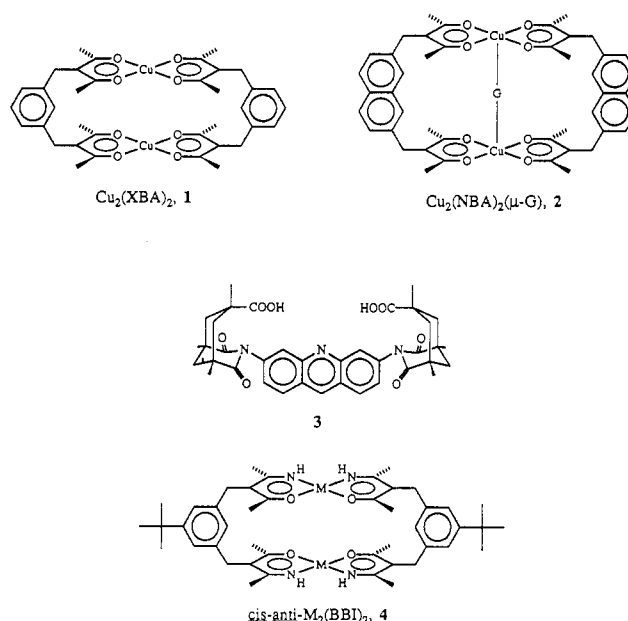
Introduction

Since our initial report of the cofacial binuclear bis(β -diketone) complex $Cu_2(XBA)_2$ (1; see Chart I),¹ we have been exploring the use of these and related complexes to bind guest molecules. We showed that the larger complex $Cu_2(NBA)_2$ binds guest molecules G (see 2) such as Dabco (1,4-diazabicyclo[2.2.2]octane) in an intramolecular fashion.² The resulting host-guest complex is similar to those produced by several flexible binucleating macrocycles,³ but our rigid 2,7-naphthalenediylbis(methylene) bridging groups provide a cavity of well-defined size and shape. We also examined pyrazine, whose lower basicity⁴ and larger N...N distance⁵ are likely to make intramolecular complexation less favorable.

Pyrazines and Dabco have been used to join mononuclear species to produce binuclear complexes of a variety of metals.⁶ One-,^{6b,7} two-⁸ and three-dimensional⁹ polymeric complexes have also been prepared from these diamines. The recognition of pyrazine by organic systems such as the rigid chelating diacid 3 has been studied by both experimental¹⁰ and theoretical¹¹ methods.

We now report the demonstration by X-ray analysis that pyrazines bind intramolecularly to the discrete binuclear complex $Cu_2(NBA)_2$. Coordination of substituted pyrazines to $Cu_2(NBA)_2$ is generally weaker than that of the parent compound. However, aminopyrazine binds much more strongly, probably because it can

Chart I



hydrogen-bond to the O atoms of the coordinated bis(β -diketone) ligands.

† Ligand abbreviations: acacH = 2,4-pentanedione; $XBAH_2 = m$ -xylylenebis(acetylacetonate) (3,3'-[1,3-phenylenebis(methylene)]bis(2,4-pentanedione)); $NBAH_2 = 2,7$ -naphthalenediylbis(methylene)bis(acetylacetonate) (3,3'-[2,7-naphthalenediylbis(methylene)]bis(2,4-pentanedione)); $BBIH_2 = 5$ -tert-butyl-*m*-xylylenebis(acetylacetonate imine) (3,3'-[5-(1,1-dimethylethyl)-1,3-phenylenebis(methylene)]bis(4-amino-3-penten-2-one)).

(1) Maverick, A. W.; Klavetter, F. E. *Inorg. Chem.* **1984**, *23*, 4129-4130.
(2) Maverick, A. W.; Buckingham, S. C.; Bradbury, J. R.; Yao, Q.; Stanley, G. G. *J. Am. Chem. Soc.* **1986**, *108*, 7430-7431.

Experimental Section

Materials and Procedures. Pyrazine and its derivatives were obtained from the Aldrich Chemical Co. and were used without further purification, except for chloropyrazine, which was dried by dissolving in CH_2Cl_2 , treating with Na_2SO_4 , and removing the solvent under vacuum. *tert*-Butyl alcohol (Mallinckrodt) was purified by treatment with potassium metal and subsequent distillation. All other materials were reagent or spectrophotometric grade and were used as received.

Electronic absorption spectra were recorded with use of Cary 219 and Cary 14 spectrophotometers. Binding constants were determined by using CHCl_3 solutions ca. 0.002 M in $\text{Cu}_2(\text{NBA})_2$, with maximum concentrations of added ligand L chosen so as to cause 50–75% conversion to $\text{Cu}_2(\text{NBA})_2 \cdot \text{L}$ whenever possible. Equilibrium constants were calculated from electronic spectra of solutions with several different L concentrations, using the method of Rose and Drago.¹²

NBAH₂ (3,3'-(2,7-naphthalenediylbis(methylene))bis(2,4-pentanedione)) was prepared by the general nucleophilic substitution method of Martin and co-workers,¹³ using the following quantities: 2,4-pentanedione, 3.96 g (0.0396 mol); potassium, 1.02 g (0.0264 mol); 2,7-bis-(bromomethyl)naphthalene,¹⁴ 4.17 g (0.0132 mol); KI, 0.52 g (0.0031 mol); *t*-BuOH, 100 mL. The mixture was acidic to moist litmus, indicating complete reaction, ca. 4 h after the addition of KI. Removal of three-fourths of the solvent left a semisolid residue, which was taken up in a mixture of H_2O and CH_2Cl_2 . The organic layer was washed several times with water, dried (Na_2SO_4), and evaporated to give an orange-brown liquid. Excess acetylacetone was removed from this liquid under dynamic vacuum at room temperature (ca. 48 h), leaving a thick syrup; yield 3.8 g (82%). This material was essentially pure, as judged by its ¹H NMR spectrum, and could be used directly in the synthesis of $\text{Cu}_2(\text{NBA})_2$. The syrup also solidified partially over a period of several weeks, and analytically pure white powdery NBAH₂ could be isolated from it by trituration with methanol. Anal. Calcd for NBAH₂ ($\text{C}_{22}\text{H}_{24}\text{O}_4$): C, 74.98; H, 6.86. Found: C, 75.12; H, 6.86.

$\text{Cu}_2(\text{NBA})_2 \cdot 2\text{CHCl}_3$. A solution of NBAH₂ (0.05–0.2 M) in CHCl_3 was shaken in a separatory funnel with a 10-fold excess of Cu-

Table I. Crystal Data for $\text{Cu}_2(\text{NBA})_2(\mu\text{-}2,5\text{-Me}_2\text{pyz}) \cdot 4\text{CH}_2\text{Cl}_2^a$

chem formula	$\text{Cu}_2\text{C}_{54}\text{H}_{60}\text{N}_2\text{O}_8\text{Cl}_8$	space group	$\text{C}2/m$, No. 12
fw	1275.79	temp/°C	21 ± 2
<i>a</i> /Å	22.941 (6)	$\lambda/\text{Å}$	1.54184 (Cu K α)
<i>b</i> /Å	22.432 (4)	$\rho_{\text{obsd}}, \rho_{\text{calcd}}/\text{g cm}^{-3}$	1.42 (2), 1.422
<i>c</i> /Å	11.677 (2)	$\mu(\text{Cu K}\alpha)/\text{cm}^{-1}$	46.7
β/deg	97.32 (2)	transm coeff	0.9342–0.9982
<i>V</i> /Å ³	5960 (4)	$R(F_o)$	0.096
<i>Z</i>	4	$R_w(F_o)$	0.093

^a Values in parentheses in Tables I–IV are estimated standard deviations of the last digit.

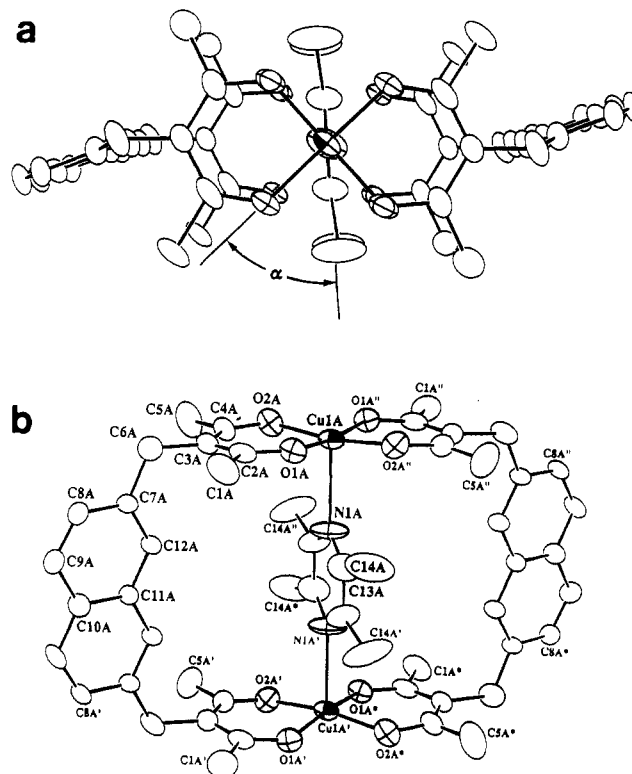


Figure 1. ORTEP¹⁸ drawings for $\text{Cu}_2(\text{NBA})_2(\mu\text{-}2,5\text{-Me}_2\text{pyz})$, molecule A, with ellipsoids at the 33% probability level: (a) top view, showing orientation of disordered 2,5-dimethylpyrazine guest molecule (as described by torsion angle α , O1A–Cu1A–N1A–C13A) and tilting of naphthalene planes; (b) side view, including atom-labeling scheme. The prime, double prime, and asterisk symbols represent atoms related to the original atoms by the operations *m*, 2, and $\bar{1}$, respectively.

- See, for example: Hoshino, N.; Jircitano, A.; Busch, D. H. *Inorg. Chem.* **1988**, *27*, 2292–2300. Coughlin, P. K.; Lippard, S. J. *Inorg. Chem.* **1984**, *23*, 1446–1451. Agnus, Y.; Louis, R.; Weiss, R. *J. Am. Chem. Soc.* **1979**, *101*, 3381–3384. Drew, M. G. B.; McCann, M.; Nelson, S. M. *J. Chem. Soc., Chem. Commun.* **1979**, 481–482.
- pK_a* values in H_2O : pyrazine, 0.65; pyridine, 5.25. Weast, R. C., Ed. *CRC Handbook of Chemistry and Physics*; CRC Press: Boca Raton, FL, 1981; p D-140.
- The N---N distances in the free amines are as follows. Dabco, 2.54 Å; Nimmo, J. K.; Lucas, B. W. *Acta Crystallogr., Sect. B* **1976**, *32*, 348–353. Pyrazine, 2.77 Å; Wheatley, P. J. *Acta Crystallogr.* **1957**, *10*, 182–187.
- (a) Durley, R. C. E.; Hughes, D. L.; Truter, M. R. *Acta Crystallogr., Sect. B* **1980**, *36*, 2991–2997. (b) Belford, R. C. E.; Fenton, D. E.; Truter, M. R. *J. Chem. Soc., Dalton Trans.* **1974**, 17–24. (c) Rudzinski, W.; Shiro, M.; Fernando, Q. *Anal. Chem.* **1975**, *47*, 1194–1196. (d) Maverick, A. W.; Ivie, M. L.; Fronczek, F. R. *Acta Crystallogr., Sect. C*, in press. (e) Albinati, A.; Isaia, F.; Kaufmann, W.; Sorato, C.; Venanzi, L. M. *Inorg. Chem.* **1989**, *28*, 1112–1122. (f) Creutz, C. *Prog. Inorg. Chem.* **1983**, *30*, 1–73. Fürholz, U.; Joss, S.; Bürgi, H.-B.; Ludi, A. *Inorg. Chem.* **1985**, *24*, 943–948. (g) Newkome, G. R.; Kohli, D. K.; Fronczek, F. R. *J. Am. Chem. Soc.* **1982**, *104*, 994–998. (h) Rao, V. M.; Sathyanarayana, D. N.; Manohar, H. *J. Chem. Soc., Dalton Trans.* **1983**, 2167–2173. (i) Bino, A.; Lay, P. A.; Taube, H.; Wishart, J. F. *Inorg. Chem.* **1985**, *24*, 3969–3971.
- Kubel, F.; Strähle, J. Z. *Naturforsch., B* **1981**, *B36*, 441–446. Cotton, F. A.; Felthouse, T. R. *Inorg. Chem.* **1981**, *20*, 600–608. Cotton, F. A.; Felthouse, T. R. *Inorg. Chem.* **1980**, *19*, 328–331. Morosin, B.; Hughes, R. C.; Soos, Z. G. *Acta Crystallogr., Sect. B* **1975**, *31*, 762–770. Valentine, J. S.; Silverstein, A. J.; Soos, Z. G. *J. Am. Chem. Soc.* **1974**, *96*, 97–103. Brodersen, K.; Hacke, N.; Liehr, G. Z. *Anorg. Allg. Chem.* **1974**, *409*, 1–10. Belford, R. C. E.; Fenton, D. E.; Truter, M. R. *J. Chem. Soc., Dalton Trans.* **1972**, 2208–2213. Vranka, R. G.; Amma, E. L. *Inorg. Chem.* **1966**, *5*, 1020–1025.
- Darriet, J.; Haddad, M. S.; Duesler, E. N.; Hendrickson, D. N. *Inorg. Chem.* **1979**, *18*, 2679–2686. Haynes, J. S.; Rettig, S. J.; Sams, J. R.; Thompson, R. C.; Trotter, J. *Can. J. Chem.* **1987**, *65*, 420–426.
- Lumme, P.; Lindroos, S.; Lindell, E. *Acta Crystallogr., Sect. C* **1987**, *43*, 2053–2056.
- Rebek, J., Jr.; Askew, B.; Killoran, M.; Nemeth, D.; Lin, F.-T. *J. Am. Chem. Soc.* **1987**, *109*, 2426–2431.
- Jorgensen, W. L.; Boudon, S.; Nguyen, T. B. *J. Am. Chem. Soc.* **1989**, *111*, 755–757.
- Rose, N. J.; Drago, R. S. *J. Am. Chem. Soc.* **1959**, *81*, 6138–6141.
- Martin, D. F.; Fernelius, W. C.; Shamma, M. *J. Am. Chem. Soc.* **1959**, *81*, 130–133.
- Prepared from 2,7-dimethylnaphthalene (Wolinska-Mocydla, J.; Cannon, P.; Leitch, L. C. *Synthesis* **1974**, 566–568) by the method of: Katz, T. J.; Ślusarek, W. *J. Am. Chem. Soc.* **1979**, *101*, 4259–4267.

(NH_3)₄²⁺(aq). The dark olive green organic layer was dried (Na_2SO_4), filtered, and evaporated to dryness. The residue was rinsed with benzene to remove brown impurities and dissolved in the minimum volume of CHCl_3 , and the solution was layered with CH_3CN or benzene, which caused crystalline $\text{Cu}_2(\text{NBA})_2 \cdot 2\text{CHCl}_3$ to be deposited over a period of several days. This deposit could be rinsed with benzene to remove brown impurities if necessary; yield 40–50%. Microanalyses of this material (C, H, Cl) corresponded to $\text{Cu}_2(\text{NBA})_2 \cdot x\text{CHCl}_3$ ($0 \leq x \leq 2$), with freshly prepared samples showing the highest Cl content and samples washed with benzene the lowest. Freshly prepared material was used to determine accurate extinction coefficients for measurement of equilibrium constants.

Adducts of $\text{Cu}_2(\text{NBA})_2$ with Lewis Bases. Solutions of $\text{Cu}_2(\text{NBA})_2 \cdot 2\text{CHCl}_3$ in CHCl_3 or CH_2Cl_2 quickly turned turquoise on treatment with a variety of pyrazine and pyridine derivatives. Most of these adducts were studied only in solution. No spectroscopic evidence for adduct formation was observed with the bases 2,6-dimethylpyridine, 2,3,5-trimethylpyrazine, 2,3,5,6-tetramethylpyrazine, and phenazine. Similarly, only $\text{Cu}_2(\text{NBA})_2 \cdot 2\text{CHCl}_3$ was formed when NBAH₂ and $\text{Cu}(\text{NH}_3)_4^{2+}$ were mixed in the presence of excess tetramethylpyrazine or phenazine or when $\text{Cu}(\text{OAc})_2 \cdot \text{H}_2\text{O}$ and NBAH₂ were mixed in neat trimethylpyrazine.

X-ray Analysis of $\text{Cu}_2(\text{NBA})_2(\mu\text{-}2,5\text{-Me}_2\text{pyz}) \cdot 4\text{CH}_2\text{Cl}_2$. We first attempted to crystallize the adduct of $\text{Cu}_2(\text{NBA})_2$ with pyrazine itself. Despite repeated attempts with a variety of solvents, we could not obtain crystals of this complex suitable for X-ray analysis. However, the adduct

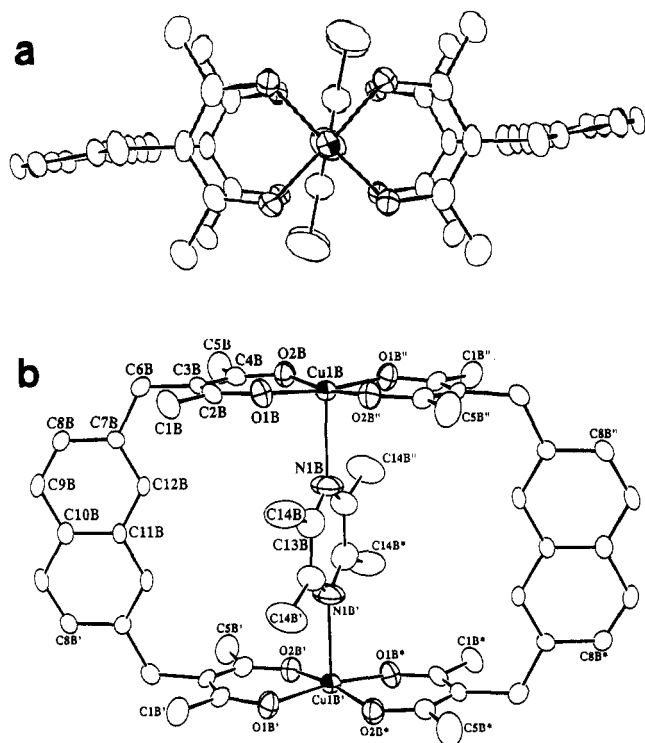


Figure 2. ORTEP¹⁸ drawings for $\text{Cu}_2(\text{NBA})_2(\mu\text{-}2,5\text{-Me}_2\text{pyz})$, as in Figure 1 except depicting molecule B.

with 2,5-dimethylpyrazine (2,5-Me₂pyz) was more readily crystallized, by layering a solution of $\text{Cu}_2(\text{NBA})_2 \cdot 2\text{CHCl}_3$ in CH_2Cl_2 first with benzene- CH_2Cl_2 (1:1 v/v) and then with pure liquid 2,5-Me₂pyz. After 24–48 h, deep turquoise parallelepipeds had formed. The crystals became opaque in less than 60 s when exposed to the atmosphere, probably due to rapid loss of CH_2Cl_2 ; therefore, they were transferred along with the mother liquor to glass capillaries that were then flame-sealed. Satisfactory microanalytical data could not be obtained for the complex because of solvent loss.

Diffraction data were collected on an Enraf-Nonius CAD4 diffractometer fitted with Cu K α source and graphite monochromator, using the θ - 2θ scan method. Final unit cell constants were determined from the orientations of 25 centered high-angle reflections. The intensities were corrected for absorption using ψ -scan data for five reflections. Additional crystallographic data are summarized in Table I; further data collection and refinement parameters are available as supplementary material.

The structure was solved by using a combination of heavy-atom and direct methods (SHELXS86¹⁵), which located the two Cu atoms and several other non-hydrogen atoms. The remaining non-hydrogen atoms were located in subsequent cycles of full-matrix least-squares refinement and difference Fourier syntheses, using the VAXSDP¹⁶ set of programs. Positional and anisotropic displacement parameters were refined for all non-hydrogen atoms; hydrogen atoms were placed in calculated positions, with fixed isotropic displacement parameters. At least one hydrogen atom in each methyl group was located in the difference maps. These positions were used as guides in determining the conformations of the methyl groups. The resulting O-C-C-H torsion angles at C1A, C5A, C1B, and C5B, -4, -8, -19, and 0°, respectively, reflect approximately eclipsed O-C-C-H conformations. We found similar methyl group conformations in $\text{Cu}_2(\text{XBA})_2$ ¹ and $\text{Cu}_2(\text{NBA})_2 \cdot 2\text{CHCl}_3$ ² and in the bis-(β -keto enamine) complexes $\text{M}_2(\text{BBI})_2$ (4).¹⁷

There are four independent CH_2Cl_2 molecules in the structure, with a total occupancy of 4 per $\text{Cu}_2(\text{NBA})_2$ unit. C11-C1Cl-C12 is in a general position. The second and third CH_2Cl_2 molecules lie on or near mirror planes and are disordered. No carbon atom could be found for the third CH_2Cl_2 molecule, but the C15---C16 distance (2.51 (2) Å) is reasonable. The fourth CH_2Cl_2 molecule, which lies at a 2/m site, was

Table II. Atomic Coordinates for $\text{Cu}_2(\text{NBA})_2(\mu\text{-}2,5\text{-Me}_2\text{pyz}) \cdot 4\text{CH}_2\text{Cl}_2$

atom	x	y	z	$B_{\text{eqv}}/\text{Å}^2$ ^a
Cu1A	0	0.33070 (8)	0	3.79 (4)
O1A	0.0048 (2)	0.3251 (3)	-0.1618 (4)	4.4 (1)
O2A	-0.0839 (2)	0.3236 (3)	-0.0277 (4)	4.9 (2)
C1A	-0.0172 (4)	0.3278 (5)	-0.3629 (7)	5.7 (3)
C2A	-0.0384 (4)	0.3274 (4)	-0.2434 (6)	4.3 (2)
C3A	-0.0981 (4)	0.3300 (4)	-0.2324 (6)	3.8 (2)
C4A	-0.1180 (4)	0.3281 (4)	-0.1243 (7)	4.3 (2)
C5A	-0.1823 (4)	0.3304 (5)	-0.1096 (8)	7.1 (3)
C6A	-0.1406 (5)	0.3322 (4)	-0.3399 (7)	5.2 (2)
C7A	-0.1500 (4)	0.3911 (3)	-0.4005 (7)	3.5 (2)
C8A	-0.1717 (4)	0.3922 (4)	-0.5192 (7)	3.8 (2)
C9A	-0.1834 (4)	0.4436 (4)	-0.5759 (7)	4.3 (2)
C10A	-0.1714 (5)	1/2	-0.5205 (9)	3.8 (3)
C11A	-0.1491 (5)	1/2	-0.4007 (9)	3.1 (3)
C12A	-0.1374 (4)	0.4441 (4)	-0.3451 (6)	3.5 (2)
N1A	0	0.4400 (4)	0	6.6 (3)
C13A	0.0395 (4)	0.4698 (4)	-0.0450 (8)	6.0 (3)
C14A ^b	0.095 (1)	0.448 (1)	-0.097 (2)	10.3 (7)
Cu1B	0	0.16849 (8)	1/2	3.39 (4)
O1B	-0.0040 (2)	0.1752 (3)	0.6629 (4)	4.3 (1)
O2B	-0.0838 (2)	0.1756 (3)	0.4661 (4)	4.1 (1)
C1B	-0.0377 (4)	0.1701 (4)	0.8429 (7)	4.9 (2)
C2B	-0.0504 (4)	0.1722 (4)	0.7138 (6)	3.6 (2)
C3B	-0.1080 (3)	0.1708 (3)	0.6585 (7)	3.3 (2)
C4B	-0.1212 (4)	0.1727 (4)	0.5383 (7)	4.0 (2)
C5B	-0.1842 (4)	0.1722 (5)	0.4812 (8)	6.1 (3)
C6B	-0.1577 (4)	0.1683 (4)	0.7331 (7)	4.3 (2)
C7B	-0.1767 (3)	0.1084 (3)	0.7724 (6)	3.2 (2)
C8B	-0.2158 (3)	0.1071 (4)	0.8573 (6)	3.2 (2)
C9B	-0.2356 (3)	0.0559 (4)	0.8946 (6)	3.4 (2)
C10B	-0.2165 (5)	0	0.8562 (9)	3.0 (3)
C11B	-0.1773 (5)	0	0.7723 (8)	2.7 (2)
C12B	-0.1570 (3)	0.0555 (4)	0.7349 (6)	3.3 (2)
N1B	0	0.0626 (5)	1/2	6.3 (3)
C13B	0.0235 (4)	0.0312 (4)	0.5870 (7)	5.3 (3)
C14B ^b	0.055 (1)	0.057 (1)	0.708 (2)	8.3 (7)
C11	0.3276 (2)	0.2179 (2)	0.2333 (3)	9.5 (1)
C12	0.3536 (2)	0.3217 (2)	0.1063 (3)	9.9 (1)
C1Cl	0.3827 (4)	0.2646 (4)	0.1955 (8)	5.2 (3)
C13	0.3220 (3)	1/2	0.4317 (5)	13.8 (2)
C14	0.2804 (4)	1/2	0.1999 (6)	23.9 (5)
C2Cl	0.293 (1)	0.461 (1)	0.305 (2)	11.3 (8)
C15 ^c	0.4843 (5)	0	0.352 (1)	12.5 (4)
C16 ^c	0.5239 (5)	0	0.562 (1)	17.5 (6)
LC ^d	0.4629 (4)	1/2	0.974 (1)	16.4 (4)
C18 ^c	0.4198 (7)	0.4522 (6)	1.044 (1)	10.6 (5)

^aThe isotropic equivalent displacement parameter B_{eqv} is defined as $\frac{1}{3}(a^2\beta_{11} + b^2\beta_{22} + c^2\beta_{33} + ac\beta_{13} \cos \beta)$. ^bThe disordered methyl groups in the 2,5-dimethylpyrazine moieties were assigned 1/2 occupancy. ^cTotal occupancy 1/2 (i.e. 2 molecules per unit cell). ^dSuperposed C and Cl atoms, each with occupancy 1/2 and coordinates and displacement parameters constrained to be equal.

Table III. Selected Interatomic Distances/Å for $\text{Cu}_2(\text{NBA})_2(\mu\text{-}2,5\text{-Me}_2\text{pyz}) \cdot 4\text{CH}_2\text{Cl}_2$ ^a

	mol A	mol B	mol A	mol B
Cu1---Cu1'	7.596 (2)	7.559 (2)	C3-C4	1.396 (7)
Cu1-O1	1.910 (3)	1.922 (3)	C3-C6	1.489 (7)
Cu1-O2	1.918 (4)	1.920 (4)	C4-C5	1.508 (8)
Cu1-N1	2.452 (7)	2.374 (7)	C6-C7	1.500 (7)
O1-C2	1.285 (6)	1.286 (6)	N1-C13	1.290 (7)
O2-C4	1.292 (6)	1.280 (6)	C13-C13'	1.35 (1)
C1-C2	1.536 (7)	1.499 (7)	C13-C14	1.55 (1)
C2-C3	1.393 (8)	1.395 (7)	C14---C14'	2.31 (3) ^b
				2.55 (3) ^b

^aThe headings "mol A" and "mol B" in Tables III and IV indicate corresponding values for the two independent molecules in the structure. The prime and double prime symbols represent atoms related to the original atoms by the crystallographic symmetry operations m and 2 , respectively. ^bThese distances are unrealistically short due to the rotational disorder (Figure 4) of the 2,5-Me₂pyz moieties; see text for details.

modeled with one Cl atom (C18) and one atom (LC) which consists of superposed C and Cl atoms, with coordinates and displacement parameters constrained to be equal. An illustration of the disorder model for this fourth CH_2Cl_2 molecule is included as supplementary material.

- (15) Sheldrick, G. M. In *Crystallographic Computing 3*; Sheldrick, G. M., Krüger, C., Goddard, R., Eds.; Oxford University Press: Oxford, England 1985; pp 175–189.
- (16) Frenz, B. A. *Enraf-Nonius Structure Determination Package*; Enraf-Nonius: Delft, The Netherlands, 1985.
- (17) Bradbury, J. R.; Hampton, J. L.; Martone, D. P.; Maverick, A. W. *Inorg. Chem.* **1989**, *28*, 2392–2399.

Table IV. Selected Bond Angles/deg for $\text{Cu}_2(\text{NBA})_2(\mu\text{-}2,5\text{-Me}_2\text{pyz})\cdot 4\text{CH}_2\text{Cl}_2$

	mol A	mol B		mol A	mol B
O1-Cu1-O1''	172.5 (2)	171.0 (2)	C2-C3-C6	118.0 (5)	118.0 (5)
O1-Cu1-O2	90.6 (2)	91.4 (2)	C4-C3-C6	120.6 (6)	119.6 (5)
O1-Cu1-O2''	88.7 (2)	87.8 (2)	O2-C4-C3	124.1 (6)	125.8 (6)
O1-Cu1-N1	93.8 (1)	94.5 (1)	O2-C4-C5	113.2 (5)	113.1 (5)
O2-Cu1-O2''	170.5 (2)	170.5 (2)	C3-C4-C5	122.6 (5)	121.0 (5)
O2-Cu1-N1	94.7 (1)	94.8 (1)	C3-C6-C7	117.8 (5)	118.4 (4)
Cu1-O1-C2	126.5 (4)	126.9 (4)	Cu1-N1-C13	121.2 (4)	123.0 (4)
Cu1-O2-C4	128.5 (4)	126.8 (4)	C13-N1-C13''	117.6 (8)	114.1 (8)
O1-C2-C1	111.8 (6)	113.6 (5)	N1-C13-C13'	121.2 (4)	123.0 (4)
O1-C2-C3	127.4 (5)	125.4 (5)	N1-C13-C14	130.6 (7) ^a	126.1 (7) ^a
C1-C2-C3	120.9 (5)	121.1 (5)	C13'-C13-C14	108.0 (5) ^a	111.0 (5) ^a
C2-C3-C4	121.4 (5)	122.3 (5)			

^a Angles involving C14 are distorted due to the rotational disorder (Figure 4) of the 2,5-Me₂pyz moieties; see text for details.

Refinement converged at $R = 0.096$ ($R_w = 0.093$) for 372 parameters and 3358 reflections with $I > 1\sigma(I)$. Figures 1 and 2 are ORTEP¹⁸ drawings for the two independent molecules. Refined atomic positional parameters and selected bond lengths and angles are presented in Tables II-IV.

Because the space group for $\text{Cu}_2(\text{NBA})_2(\mu\text{-}2,5\text{-Me}_2\text{pyz})\cdot 4\text{CH}_2\text{Cl}_2$ was not uniquely determined from the diffraction data, we also attempted to refine models in the lower symmetry space groups $C2$ and Cm . (Neither of these subgroups is compatible with a fully ordered 2,5-dimethylpyrazine moiety. Thus, these refinements were not expected to yield new chemical information. Still, some improvement might have been possible in the disordered solvent molecules.) For each of these attempts, starting coordinates for the non-hydrogen atoms were taken from the $C2/m$ structure, with small shifts (maximum 0.05 Å) in randomly chosen directions to break the higher symmetry. The refinements led to unreasonable and irregular distances in the $\text{Cu}_2(\text{NBA})_2(\mu\text{-}2,5\text{-Me}_2\text{pyz})$ moieties. Also, large correlation coefficients were observed in these refinements between parameters related by the symmetry elements that had been removed (e.g. mirror-related parameters in the $C2$ trial.) Therefore, $C2/m$ is better than the lower symmetry space groups for this structure.

The presence of two molecules in the asymmetric unit, both on special positions, raised the possibility that a higher symmetry space group (which might include a glide plane or screw axis relating the two molecules) had been overlooked. However, this is unlikely, for the following reasons. First, the program TRACER¹⁶ found no higher symmetry unit cells. Second, the conformations of the two molecules are substantially different, especially in the orientation of the naphthalenediyl bridges and the 2,5-dimethylpyrazine guests (see discussion of least-squares plane orientations below and "top views" in Figures 1 and 2). Third, although some of the atoms in molecules A and B appear to be related by the relatively simple transformation $(x, 1/2 - y, 1/2 - z)$, this transformation fails for atoms such as C5 and C14. And finally, during least-squares refinement, no correlation coefficients greater than 0.5 were observed between parameters describing the two molecules. These observations make it extremely unlikely that we have overlooked additional symmetry in this structure.

Results

Synthesis of NBAH₂ and Its Complexes. The preparation of NBAH₂ from 2,7-bis(bromomethyl)naphthalene resembles our previous methods for bis(β-diketones), which are based on the general procedure of Martin and co-workers.¹³ Treating a solution of NBAH₂ in CH₂Cl₂ or CHCl₃ with $\text{Cu}(\text{NH}_3)_4^{2+}(\text{aq})$ produces $\text{Cu}_2(\text{NBA})_2$. This olive green complex and its turquoise adducts with Lewis bases are soluble in CHCl₃ and slightly soluble in other chlorinated hydrocarbons. Some of the adducts could be isolated as solids; the others, especially those that are more weakly bound, were studied only in solution.

Binding of Lewis Bases. The electronic spectrum of $\text{Cu}_2(\text{NBA})_2$ (see trace 1 in Figure 3) closely resembles those of $\text{Cu}(\text{acac})_2$ and the smaller binuclear complex $\text{Cu}_2(\text{XBA})_2$,¹ the bands in the 450–800-nm region are due to d-d transitions. The difference in color between $\text{Cu}(\text{acac})_2$ (blue-gray) and the binuclear species (olive green) is attributable to the steeply increasing absorption below 470 nm for the binuclear complexes. Olive green solutions

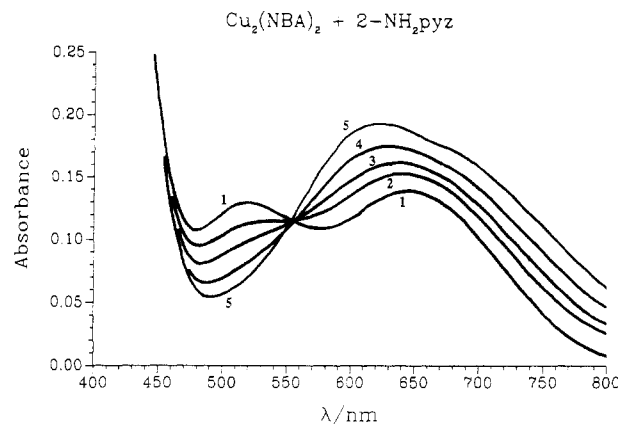


Figure 3. Electronic absorption spectra of $\text{Cu}_2(\text{NBA})_2$ (0.00179 M) in CHCl_3 at room temperature, with the following concentrations of added 2-aminopyrazine: trace 1, 0 M; trace 2, 0.00276 M; trace 3, 0.00552 M; trace 4, 0.0110 M; trace 5, 0.0221 M.

Table V. Binding Constants for $\text{Cu}_2(\text{NBA})_2$ with Amines^a

amine	K/M^{-1}	amine	K/M^{-1}
Dabco	220 ^b	pyridine (py)	0.5 ^b
pyrazine (pyz)	5 ^b	2-Mepy	<0.2 ^c
2-Mepyz	2.8	4-Mepy	0.5
2,3-Me ₂ pyz	0.26	3,5-Me ₂ py	0.6
2,5-Me ₂ pyz	0.83	2-NH ₂ py	1.0
2,3-Et ₂ pyz	<0.2 ^c	4-Me ₂ Npy	2.6
2-NH ₂ pyz	93		
2-CH ₃ Opyz	0.3 ^c		
2-Cl-pyz	0.3 ^c		
quinoxaline	0.7		

^a In CHCl_3 , 25 ± 2 °C. ^b Reference 3. ^c Value difficult to measure (estimated uncertainty $\pm 50\%$); other values were generally reproducible within $\pm 10\%$.

of $\text{Cu}_2(\text{NBA})_2$ turn turquoise on addition of nitrogenous bases. Spectra measured in a typical experiment, involving $\text{Cu}_2(\text{NBA})_2$ and increasing amounts of 2-aminopyrazine, are illustrated in Figure 3. We used these electronic spectral changes to determine the binding constants listed in Table V. The calculations utilized absorbance changes at 500 and 600 nm, because these wavelengths generally led to the largest decreases and increases in absorbance, respectively. (Using absorbance data at other wavelengths yielded similar binding constants.)

Structure of $\text{Cu}_2(\text{NBA})_2(\mu\text{-}2,5\text{-Me}_2\text{pyz})\cdot 4\text{CH}_2\text{Cl}_2$. X-ray analysis of this compound demonstrates that pyrazines coordinate intramolecularly to $\text{Cu}_2(\text{NBA})_2$. The crystals contain two crystallographically independent binuclear units (see Figures 1 and 2), each of which lies at a site of $2/m$ (C_{2h}) symmetry. The Cu atoms and the 2,5-dimethylpyrazine N atoms lie parallel to b , on the 2-fold axes, and atoms C10 and C11 in the naphthalene moieties lie in mirror planes. The symmetry of the $\text{Cu}_2(\text{NBA})_2(\mu\text{-}2,5\text{-Me}_2\text{pyz})$ sites requires that the 2,5-Me₂pyz moieties be disordered; their methyl groups and aromatic H atoms are

(18) Johnson, C. K. ORTEP-II: A Fortran Thermal-Ellipsoid Plot Program for Crystal-Structure Illustrations; Report ORNL-5138; National Technical Information Service, U.S. Department of Commerce: Springfield, VA, 1976.

assigned occupancies of $1/2$. (The structure of the unsubstituted analogue, $\text{Cu}_2(\text{NBA})_2(\mu\text{-pyz})$, would not exhibit this type of disorder. However, we could not obtain crystals of $\text{Cu}_2(\text{NBA})_2(\mu\text{-pyz})$ suitable for X-ray analysis.)

The top views of the complexes in Figures 1 and 2 illustrate the orientations of the 2,5- Me_2pyz guest molecules, with their methyl groups pointed outward from the complex. The torsion angles O1-Cu1-N1-C13 , shown as α , are -51.2 (5°) in molecule A and -32.2 (5°) in molecule B. Also visible is the tilting of the naphthalene moieties, which can be estimated by comparing two planes: one defined by the atoms C7-C12 and the second defined by the four atoms C6. The normals to these planes make an angle of 20.2 (4°) in molecule A and 8.4 (9°) in molecule B.

The $\text{Cu}_2(\text{NBA})_2(\mu\text{-2,5-Me}_2\text{pyz})$ molecules are arranged in layers perpendicular to b , with a distance of ca. 3.4 \AA separating the $\text{Cu}(\text{acac})_2$ moieties of adjacent layers (the shortest significant distance between layers is $\text{C2A} \cdots \text{C2B} = 3.524 \text{ \AA}$). This close approach suggests a weak π interaction between adjacent molecules, of the type we have observed previously in $\text{Cu}_2(\text{NBA})_2 \cdot 2\text{CHCl}_3$ (intermolecular contacts $3.22\text{--}3.25 \text{ \AA}$) and $\text{Cu}_2(\text{NBA})_2(\mu\text{-Dabco}) \cdot 2\text{CH}_2\text{Cl}_2 \cdot 2\text{H}_2\text{O}$.² Within the layers in $\text{Cu}_2(\text{NBA})_2(\mu\text{-2,5-Me}_2\text{pyz}) \cdot 4\text{CH}_2\text{Cl}_2$, the orientations of the A and B molecules are approximately perpendicular: normals to the least-squares planes defined by the four atoms C6 in the two molecules make an angle of 89.6 (1°). The closest intermolecular contacts within the layers are $\text{H9A} \cdots \text{C9B} = 3.00 \text{ \AA}$ and $\text{H4A3} \cdots \text{H9B} = 2.50 \text{ \AA}$. The disordered solvent molecules represented by C15, C16 and C18, LC lie between the A and B molecules, on or near the $2/m$ sites at $(1/2, 0, 1/2)$ and $(0, 0, 0)$, respectively.

Discussion

Comparison of $\text{Cu}_2(\text{NBA})_2(\mu\text{-2,5-Me}_2\text{pyz})$ with Other Structures. The $\text{Cu} \cdots \text{Cu}$ distances in the present structure (7.596 (2) \AA in molecule A; 7.559 (2) \AA in molecule B) are substantially longer than those in $\text{Cu}_2(\text{NBA})_2$ (7.349 (1) \AA) and $\text{Cu}_2(\text{NBA})_2(\mu\text{-Dabco})$ (7.401 (4) \AA).² The present $\text{Cu} \cdots \text{Cu}$ distances are similar to those spanning the 2,7-naphthalenediylbis(methylene) bridging groups ($\text{C6A} \cdots \text{C6A}' = 7.53$ (1) \AA ; $\text{C6B} \cdots \text{C6B}' = 7.55$ (1) \AA). However, the bis(β -diketone) O atoms are considerably farther apart ($7.85\text{--}7.91 \text{ \AA}$), reflecting the square-pyramidal coordination environment about Cu. These larger $\text{O} \cdots \text{O}'$ separations occur primarily because the acac moieties are bent away from the center of the complex (they make angles of 86.8 (5) and 87.1 (2) $^\circ$ with the $\text{Cu} \cdots \text{Cu}$ vector in molecules A and B, respectively). This bending is made possible in part by slightly larger naphthalene- CH_2 -acac bond angles (117.8 (5) and 118.4 (4) $^\circ$ in molecules A and B, respectively, compared to 116.0 (3) and 116.3 (3) $^\circ$ in $\text{Cu}_2(\text{NBA})_2$).

The environment about the Cu atoms in $\text{Cu}_2(\text{NBA})_2(\mu\text{-2,5-Me}_2\text{pyz})$ is square pyramidal, with the Cu atoms displaced slightly (0.141 (2) \AA in molecule A; 0.155 (2) \AA in molecule B) out of the plane of the O atoms toward the axial N atoms. These displacements are similar to that observed in $\text{Cu}_2(\text{NBA})_2(\mu\text{-Dabco})$ (0.175 (2) \AA)² but considerably smaller than those in other five-coordinate adducts of bis(β -diketonato)copper complexes: 0.27 (2) \AA in (4-picoline) $\text{Cu}(\text{o-hydroxyacetophenonato})_2$,¹⁹ 0.24 (1) \AA in $[\text{Cu}(\text{hfac})_2]_2(\mu\text{-pyz})$,^{6b} 0.251 (4), 0.271 (4), and 0.240 (4) \AA in $[\text{Cu}(\text{hfac})_2]_2(\mu\text{-Dabco})$.^{6a}

The coordinated 2,5- Me_2pyz moieties in the present structure are somewhat distorted, suggesting additional disorder. The distortion is clearest in the geometry at C13: the N1-C13-C14 angles (molecule A, 130.6 (7) $^\circ$; molecule B, 126.1 (7) $^\circ$) are significantly larger than corresponding angles in 6,6'-dimethyl-2,2'-bipyridine-3,3'-diol (116.5) $^\circ$,²⁰ $\text{Cu}(6,6'\text{-dimethyl-2,2'-bipyridine})_2^+$ ($115.7\text{--}116.9$) $^\circ$,²¹ and 2,3,5,6-tetramethylpyrazine ($117.7, 118.5$) $^\circ$.²² Also, the distances between the mirror-related

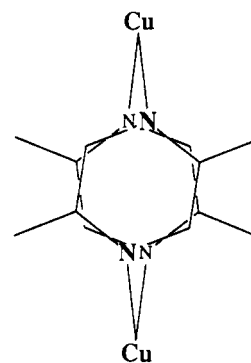


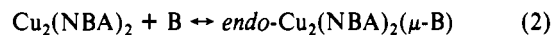
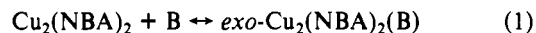
Figure 4. Schematic drawing of proposed rotational disorder for bound 2,5- Me_2pyz in the structure of $\text{Cu}_2(\text{NBA})_2(\mu\text{-2,5-Me}_2\text{pyz})$. The amount of rotational disorder has been exaggerated for clarity.

methyl C atoms ($\text{C14A} \cdots \text{C14A}' = 2.31$ (3) \AA ; $\text{C14B} \cdots \text{C14B}' = 2.55$ (3) \AA) are considerably smaller than that expected for noninterfering substituents in a six-membered ring (ca. 2.9 \AA). These features are unlikely to reflect a distortion in the 2,5- Me_2pyz molecules themselves. Instead, they probably represent rotation of bound 2,5- Me_2pyz about an axis perpendicular to the aromatic ring, so as to minimize steric repulsion between the methyl groups and the bis(β -diketone) O atoms. A schematic drawing of this rotational disorder is shown in Figure 4. According to this model, in any one $\text{Cu}_2(\text{NBA})_2(\mu\text{-2,5-Me}_2\text{pyz})$ molecule, the $\text{Cu-N} \cdots \text{N-Cu}$ linkage is nonlinear because of this rotation. The average of the two possible orientations of bound 2,5- Me_2pyz produces the observed structure, with large apparent N1-C13-C14 angles and small apparent $\text{C14} \cdots \text{C14}'$ distances.

The disorder model of Figure 4 is also supported by the relatively large displacement parameters for N1 and C13 in both molecules. Analyzing these ellipsoids is complicated somewhat by contributions from rotation about the $\text{Cu-N} \cdots \text{N-Cu}$ axis. However, projections of the ellipsoids in the pyrazine planes show substantial elongation, in directions tangent to the rings, compared to those of C7-C12 in the bridging naphthalenediyl moieties. A diagram illustrating these projections is included as supplementary material.

Thermodynamics of Endo and Exo Coordination of Lewis Bases

B. Pyridine and its derivatives can bind to the $\text{Cu}_2(\text{NBA})_2$ host only in an exo fashion. However, for difunctional guests of appropriate size, endo (intramolecular) coordination is also possible. If the guest does not cause strain in $\text{Cu}_2(\text{NBA})_2$, ΔH for endo coordination of B (eq 2) should be approximately twice as great



as that for exo coordination (eq 1). Then, because ΔS values are expected to be similar for the two reactions,²³ ΔG_2 , and the corresponding binding constant K_2 , can be substantially more favorable.

Binding of Pyrazines. Nearly all substituted pyrazines exhibit lower affinity for $\text{Cu}_2(\text{NBA})_2$ than the parent ligand. This trend is as expected on steric grounds; with bulky guest molecules, e.g. 2,3-diethylpyrazine, adduct formation is slight even in the presence of very large concentrations of the guest. Fused aromatic rings (as in quinoxaline) also inhibit binding to $\text{Cu}_2(\text{NBA})_2$.

We observed no spectroscopic evidence for binding of any of the following more highly substituted derivatives: phenazine, 2,3,5-trimethylpyrazine, and 2,3,5,6-tetramethylpyrazine. We also

(19) Duckworth, V. F.; Stephenson, N. C. *Acta Crystallogr., Sect. B* **1969**, *25*, 2245-2254.

(20) Vogt, L. H.; Wirth, J. G. *J. Am. Chem. Soc.* **1971**, *93*, 5402-5405.

(21) Burke, P. J.; McMillin, D. R.; Robinson, W. R. *Inorg. Chem.* **1980**, *19*, 1211-1214.

(22) Cromer, D. T. *J. Phys. Chem.* **1957**, *61*, 254-255. Cromer, D. T.; Ihde, A. J.; Ritter, H. L. *J. Am. Chem. Soc.* **1951**, *73*, 5587-5590. The N-C-CH_3 angles in this molecule may be decreased somewhat by repulsion between the CH_3 groups. However, the structures of the less sterically hindered 2-methylpyrazine and 2,5- and 2,6-dimethylpyrazine have not been reported.

(23) The adducts in reactions 1 and 2 can form in four and two equivalent ways, respectively, for a bidentate base B; these statistical factors lead to an increase in ΔS_1 of $5.76 \text{ J mol}^{-1} \text{ K}^{-1}$ relative to ΔS_2 .

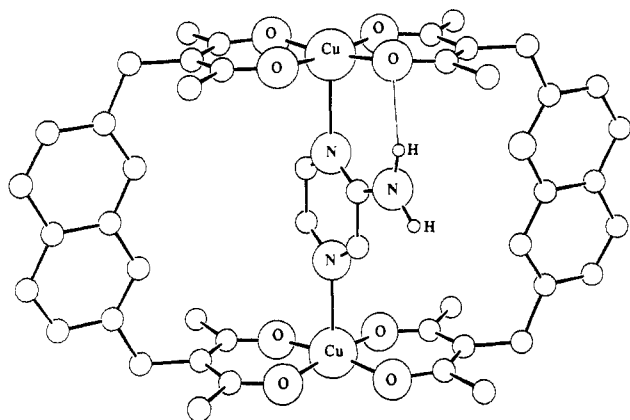


Figure 5. Proposed structure for $\text{Cu}_2(\text{NBA})_2(\mu\text{-}2\text{-NH}_2\text{pyz})$, with $\text{NH}\cdots\text{O}$ hydrogen bond indicated by a thin solid line.

Table VI. Thermodynamics of Binding to $\text{Cu}_2(\text{NBA})_2^a$

amine	$\Delta H/\text{kJ mol}^{-1}$	$\Delta S/\text{J mol}^{-1} \text{K}^{-1}$	amine	$\Delta H/\text{kJ mol}^{-1}$	$\Delta S/\text{J mol}^{-1} \text{K}^{-1}$
Dabco ^b	-30	-50	2-Mepyz	-16	-45
pyrazine	-28	-80	2-NH ₂ pyz	-29	-60

^aIn CHCl_3 , 5–35 °C. Estimated uncertainties $\pm 5 \text{ kJ mol}^{-1}$ in ΔH and $\pm 10 \text{ J mol}^{-1} \text{K}^{-1}$ in ΔS . ^bReference 2.

attempted to prepare $\text{Cu}_2(\text{NBA})_2(\mu\text{-B})$ ($\text{B} = 2,3,5$ -trimethylpyrazine, 2,3,5,6-tetramethylpyrazine) directly from Cu^{2+} , NBAH_2 , and B , again without success: only $\text{Cu}_2(\text{NBA})_2$ was isolated. The structure of $\text{Cu}_2(\text{NBA})_2(\mu\text{-}2,5\text{-Me}_2\text{pyz})$ suggests that $\text{Cu}_2(\text{NBA})_2$ could accommodate a tetrasubstituted pyrazine guest. However, this structure is deceptive because of the rotational disorder of the bound 2,5-Me₂pyz molecule (see Figure 4 and discussion above). Molecules containing adjacent methyl groups cannot relieve unfavorable steric interactions with the $\text{Cu}_2(\text{NBA})_2$ host by this rotation; therefore, their binding should be significantly less favorable. This trend is already noticeable with 2,3-dimethylpyrazine, which binds substantially less strongly than 2,5-dimethylpyrazine.

The pyrazine derivative that binds most strongly to $\text{Cu}_2(\text{NBA})_2$ is 2-aminopyrazine: the binding constant is more than 30 times as large as that for 2-methylpyrazine, which has a similar shape. No major spectroscopic differences are observed between $\text{Cu}_2(\text{NBA})_2$ solutions containing 2-aminopyrazine and those containing the other pyrazines. Therefore, like pyrazine and its other derivatives, 2-aminopyrazine probably also coordinates intramolecularly to $\text{Cu}_2(\text{NBA})_2$ via its heterocyclic N atoms. Also, molecular models indicate no plausible arrangement of metal atoms in $\text{Cu}_2(\text{NBA})_2$ that would accommodate coordination of one heterocyclic N atom and the NH_2 group. Therefore, the greatly enhanced binding must be due to a specific electronic effect rather than to a change in coordination geometry. We believe the cause is hydrogen bonding between the NH_2 group and the bis(β -diketone) O atoms. Figure 5 shows one possible geometry of $\text{Cu}_2(\text{NBA})_2(\mu\text{-NH}_2\text{pyz})$, in which the $(\text{N})\text{H}\cdots\text{O}$ distance (2.08 Å²⁴) is appropriate for hydrogen bonding.

This assignment of hydrogen bonding between 2-aminopyrazine and the coordinated bis(β -diketones) is supported further by the

results of previous NMR line-broadening^{1,25} and infrared spectral studies,²⁶ which have revealed weak interactions between various hydrogen-bond donors and metal β -diketone complexes. Also, in the crystal structure of $\text{Cu}_2(\text{NBA})_2 \cdot 2\text{CHCl}_3$,² the CHCl_3 molecules are weakly hydrogen-bonded to the bis(β -diketone) O atoms. The thermodynamic data presented in Table VI indicate that ΔH for binding of 2-aminopyrazine to $\text{Cu}_2(\text{NBA})_2$ is ca. 13 kJ mol^{-1} more favorable than that of 2-methylpyrazine. We attribute this difference primarily to $\text{NH}_2\cdots\text{O}$ hydrogen bonding. The electron-releasing amino group will make 2-aminopyrazine a better electron donor for transition-metal atoms, and this should also enhance its binding to $\text{Cu}_2(\text{NBA})_2$. However, the relatively small binding constant for 2-methoxy pyrazine suggests that this electron-releasing effect is minor.

The experimental ΔS value we found previously for binding of Dabco to $\text{Cu}_2(\text{NBA})_2$ ² is similar to that predicted if the bound Dabco molecule retains its ability to rotate about the $\text{N}\cdots\text{N}$ axis. Because rotation of bound pyrazine is only slightly more sterically restricted than that of Dabco,²⁷ we expected that the ΔS values for binding of the two bases would be similar; thus, the weaker binding of pyrazine should be primarily a result of a more positive value of ΔH . However, the data in Table VI do not support this interpretation; also, the data for the substituted pyrazines do not follow a readily explainable pattern. Thus, our previous model for the thermodynamics of intramolecular complexation may be oversimplified, and other effects, such as differences in solvation, may play a significant role even in nonpolar solvents.

Binding of Pyridines. In order to evaluate the relative importance of steric and electronic factors in binding of pyrazines to $\text{Cu}_2(\text{NBA})_2$, we also examined analogous pyridines, which can bind to $\text{Cu}_2(\text{NBA})_2$ only in the exo fashion. Substituents in the 2- and 6-positions will exert steric as well as electronic effects, whereas the influence of 3-, 4-, and 5-substituents is expected to be primarily electronic.

Methyl groups exert a slight activating effect on the binding of pyridine derivatives, except that with 2-picoline the steric repulsions clearly overwhelm any electronic effect. We observed no evidence of binding with 2,6-dimethylpyridine. Amino substituents also enhance binding in the pyridine series. With 2-aminopyridine, for example, the same type of hydrogen bonding inferred above for intramolecular coordination of 2-aminopyrazine is likely to enhance binding for exo coordination as well.

We also studied 2-(aminomethyl)pyridine (AMP), in order to determine whether its NH_2 group enhances binding to $\text{Cu}_2(\text{NBA})_2$ in a similar fashion. Although an adduct appears to form at first, the solutions gradually deposit precipitates of $[\text{Cu}(\text{AMP})_3]\text{Cl}_2$,²⁸ this prevented us from determining an accurate binding constant.

Conclusions

A variety of molecules bind intramolecularly to the cofacial binuclear complex $\text{Cu}_2(\text{NBA})_2$. Although many substituents interfere with binding of pyrazines, the amino group is substantially activating, due to hydrogen bonding with the O atoms of the coordinated β -diketones. Experiments now in progress involve the adaptation of these host-guest reactions to complexes with functionalized bridging ligands, so that chemical transformations can be performed on the bound guest molecules.

Acknowledgment is made to the donors of the Petroleum Research Fund, administered by the American Chemical Society, for support of this research. We are grateful to Professor Richard D. Gandour for numerous helpful discussions and to the reviewers

(24) The coordinates for Figure 5 were produced by the SYBYL program (Naruto, S.; Motoc, I.; Marshall, G. R.; Daniels, S. B.; Sofia, M. J.; Katzenellenbogen, J. A. *J. Am. Chem. Soc.* **1985**, *107*, 5262–5270. Clark, M.; Cramer, R. D., III; Van Opdenbosch, N. *J. Comput. Chem.*, in press, using the geometry of molecule A in the X-ray structure of $\text{Cu}_2(\text{NBA})_2(\mu\text{-}2,5\text{-Me}_2\text{pyz})$ as the starting point. The amino group in 2-aminopyrazine was assumed to be planar (as observed in 2- and 3-aminopyridine: Chao, M.; Schempp, E.; Rosenstein, R. D. *Acta Crystallogr., Sect. B* **1975**, *B31*, 2922–2924; **1975**, *B31*, 2924–2927). The conformation shown represents minimization of van der Waals energy as a function of the torsion angles about the $\text{Cu}\text{-N}$ and $\text{C}\text{-NH}_2$ bonds. A similar conformation, with $(\text{N})\text{H}\cdots\text{O} = 2.00 \text{ \AA}$, is readily accessible when the starting coordinates are those of molecule B.

(25) Kitaigorodskii, A. N.; Nekipelov, V. M.; Zamaraev, K. I. *J. Struct. Chem. (Engl. Transl.)* **1978**, *19*, 686–693.

(26) Davis, T. S.; Fackler, J. P., Jr. *Inorg. Chem.* **1966**, *5*, 242–245. Fackler, J. P., Jr. *Prog. Inorg. Chem.* **1966**, *7*, 361–425.

(27) On the basis of SYBYL calculations,²⁴ we estimate that the rotation barrier for bound pyrazine is no larger than 45 kJ mol^{-1} .

(28) This reaction appears to proceed by attack of AMP on the solvent (either CHCl_3 or CH_2Cl_2); the same material is also produced by reaction of AMP with $\text{Cu}(\text{acac})_2$: Maverick, A. W.; Ivie, M. L.; Fronczek, F. R. *J. Coord. Chem.*, in press.

for their comments. We thank Scott Buckingham for experimental assistance.

Supplementary Material Available: ORTEP illustrations of disorder in pyrazine moieties and solvent molecules and tables of crystallographic

parameters, calculated atomic coordinates, anisotropic displacement parameters, and peripheral bond distances and angles (8 pages); a listing of observed and calculated structure factors for $\text{Cu}_2(\text{NBA})_2(\mu\text{-}2,5\text{-Me}_2\text{pyz})\cdot 4\text{CH}_2\text{Cl}_2$ (9 pages). Ordering information is given on any current masthead page.

Contribution from the Department of Chemistry, D-006, University of California at San Diego, La Jolla, California 92093

Hydrolysis of Phosphodiester with Ni(II), Cu(II), Zn(II), Pd(II), and Pt(II) Complexes

Mark A. De Rosch and William C. Trogler*

Received January 6, 1989

The hydrolysis of bis(4-nitrophenyl) phosphate (**1**) is catalyzed by $\text{Ni}(\text{tren})^{2+}$ in aqueous solution at 75 °C. The activity of the catalyst remains constant for 85 turnovers and thereafter decreases. Antitumor complexes of Pd(II) and Pt(II) were also examined but did not show turnover in the hydrolysis of ethyl 4-nitrophenyl phosphate (**2**). Catalytic rate enhancement in the hydrolysis of **1** by $\text{Ni}(\text{tren})(\text{OH})(\text{OH}_2)^+$ was 1200 at pH 8.6 and of **2** by 1×10^{-4} M $\text{Pd}(\text{bpy})^{2+}$ was 49 at pH 6.0 over spontaneous hydrolysis under the same conditions. The pH-rate profile of $\text{Ni}(\text{tren})^{2+}$ -catalyzed hydrolysis of **1** shows a pH-dependent region from pH 8.0 to pH 10.8 and a pH-independent region from pH 6.0 to pH 8.0. Ni(II) complexes of tren and bpy were compared to their corresponding Cu(II) and Zn(II) analogues. The pH-rate profile of the Pd(II)- and Pt(II)-accelerated hydrolysis of **2** shows a pH dependence from pH 6.0 to pH 7.5. The rate enhancement becomes negligible with respect to spontaneous hydrolysis at alkaline pH, which is attributed to the formation of hydroxy-bridged polymers. A mechanism involving intramolecular hydroxide attack on a metal-bound phosphate is proposed. Of the $\text{M}(\text{bpy})^{2+}$ and $\text{M}(\text{tren})^{2+}$ complexes examined ($\text{M} = \text{Ni}^{2+}, \text{Cu}^{2+}, \text{Zn}^{2+}$) only the $\text{Cu}(\text{bpy})^{2+}$ complex was effective in nicking supercoiled plasmid DNA. The inhibition of DNA nicking by Ce^{4+} for the latter complex suggests that nicking occurs by a redox process rather than by hydrolysis.

Introduction

The development of artificial nucleases for use in molecular genetics and genetic engineering remains a challenging research problem because of the stability of the phosphate diester backbone and its resistivity to hydrolytic cleavage. A majority of the efforts have concentrated on the development of sequence-specific DNA binding agents attached to Fenton reagent analogues for nicking DNA.^{1,2} Fenton-like systems cut DNA through production of hydroxide radicals by a proposed mechanism that involves oxidation of the deoxyribose moiety followed by breakage of the sugar-phosphate backbone.³ Complexes that hydrolytically cleave DNA would be the preferred method for DNA cleavage, and ideally they should be catalytic. This problem reduces to effecting the hydrolytic cleavage of phosphodiester. Recently the hydrolytic cleavage of supercoiled plasmid DNA has been reported using Cu^{2+} , Zn^{2+} , Cd^{2+} , and Pb^{2+} complexed to a DNA-binding ruthenium(II) tris(phenanthroline) derivative.⁴ Nonredox-active metals such as Ni(II) and Zn(II) are potentially of interest as hydrolytic cleaving agents, and their reactivity in model systems may lead to functional DNA cleaving molecules.

Two reports exist of turnover in the hydrolysis of phosphate diesters. One is the $\text{Co}(\text{tme})_2(\text{OH})(\text{OH}_2)^{2+}$ catalyzed hydrolysis of ethyl 4-nitrophenyl methylphosphonate, which is complicated by rapid reactions of the Co(III) complex with CO_2 . This results in a short-lived catalyst.⁵ The second is the $\text{Cu}(\text{bpy})(\text{OH})(\text{OH}_2)^+$ -catalyzed hydrolysis of bis(4-nitrophenyl) phosphate to greater than 1000 turnovers.⁶ Previous examples of metal-cat-

alyzed hydrolysis of phosphate diesters were limited to substrates that contain a neighboring group, which participates in the hydrolysis.^{7,8} Metallic⁹ and nonmetallic¹⁰ micelles also accelerate the rate of hydrolysis of simple phosphate diesters. Because the presently available catalysts exhibit rates several orders of magnitude too slow to be useful in DNA hydrolysis,¹¹ a better understanding of mechanistic features might be helpful in designing more effective systems.

Many reports exist in the literature of metal ion promoted hydrolysis of phosphate monoesters^{12–14} and triesters.^{15–17} A majority of these reports are based on the hydrolysis of phosphate mono- and triesters by polyamine Co(III),^{12,13} Ir(III),¹⁵ and Rh(III)^{15a} ions as the active metal centers as either monomers or dimers. Accounts also exist of a macrocyclic Zn(II) complex catalyzed hydrolysis of diphenyl 4-nitrophenyl phosphate by an intramolecular mechanism.¹⁶ Additionally, diamine Zn(II) and diamine Cu(II) complexes have been shown to catalyze the hydrolysis of tris(4-nitrophenyl) phosphate.¹⁷ A problem that hinders

- (a) Sugiyama, H.; Xu, C.; Murugesan, N.; Hecht, S. M.; van der Marel, G. A.; van Boom, J. H. *Biochemistry* **1988**, *27*, 58–67. (b) Baker, B. F.; Dervan, P. B. *J. Am. Chem. Soc.* **1985**, *107*, 8266–8268. (c) Taylor, J. S.; Schultz, P. G.; Dervan, P. B. *Tetrahedron* **1984**, *40*, 457–465. (d) Schultz, P. G.; Taylor, J. S.; Dervan, P. B. *J. Am. Chem. Soc.* **1982**, *104*, 6861–6863. (e) Hertzberg, R. P.; Dervan, P. B. *Biochemistry* **1984**, *23*, 3934–3945.
- (a) Baker, B. F.; Dervan, P. B. *J. Am. Chem. Soc.* **1989**, *111*, 2700–2712. (b) Veal, J. M.; Rill, R. L. *Biochemistry* **1989**, *28*, 3243–3250.
- Marfey, P.; Robinson, E. *Mutat. Res.* **1981**, *86*, 155–191.
- Basile, L. A.; Raphael, A. L.; Barton, J. K. *J. Am. Chem. Soc.* **1987**, *109*, 7550–7551.
- Kenley, R. A.; Fleming, R. H.; Laine, R. M.; Tse, D.; Winterle, J. S. *Inorg. Chem.* **1984**, *23*, 1870–1876.
- Morrow, J. R.; Trogler, W. C. *Inorg. Chem.* **1988**, *27*, 3387–3394.

- (a) Chin, J.; Zou, X. *Can. J. Chem.* **1987**, *65*, 1882. (b) Steffens, J. J.; Siewers, I. J.; Benkovic, S. J. *Biochemistry* **1975**, *14*, 2431–2440.
- (a) Eichhorn, G. L.; Tarien, E.; Butzow, J. J. *Biochemistry* **1971**, *10*, 2014–2018. (b) Butzow, J. J.; Eichhorn, G. L. *Biochemistry* **1971**, *10*, 2019–2027. (c) Ikenga, H.; Inoue, Y. *Biochemistry* **1974**, *13*, 577–582.
- Menger, F. M.; Gan, L. H.; Johnson, E.; Durst, D. M. *J. Am. Chem. Soc.* **1987**, *109*, 2800–2803.
- (a) Bunton, C. A.; Ionescu, L. G. *J. Am. Chem. Soc.* **1973**, *95*, 2912–2917. (b) Buist, G. J.; Bunton, C. A.; Robinson, L.; Sepulveda, L.; Stam, M. *J. Am. Chem. Soc.* **1970**, *92*, 4073–4078.
- Chin, J.; Banaszczuk, M.; Jubian, V.; Zou, X. *J. Am. Chem. Soc.* **1989**, *111*, 186–190.
- (a) Rawji, C. H.; Milburn, R. M. *Inorg. Chim. Acta* **1988**, *150*, 227–232. (b) Jones, D. R.; Lindoy, L. F.; Sargeson, A. M. *J. Am. Chem. Soc.* **1984**, *106*, 7807–7819. (c) Jones, D. R.; Lindoy, L. F.; Sargeson, A. M. *J. Am. Chem. Soc.* **1983**, *105*, 7327–7336. (d) Anderson, B.; Milburn, R. M.; Harrowfield, J. Mac B.; Robertson, G. B.; Sargeson, A. M. *J. Am. Chem. Soc.* **1977**, *99*, 2652–2661.
- Harrowfield, J. Mac B.; Jones, D. R.; Lindoy, L. F.; Sargeson, A. M. *J. Am. Chem. Soc.* **1980**, *102*, 7733–7741.
- Herschlag, D.; Jencks, W. P. *J. Am. Chem. Soc.* **1987**, *109*, 4665–4674.
- (a) Hendry, P.; Sargeson, A. M. *Aust. J. Chem.* **1986**, *39*, 1177–1186. (b) Hendry, P.; Sargeson, A. M. *J. Chem. Soc., Chem. Commun.* **1984**, 164–165.
- (a) Breslow, R.; Singh, H. *Bioorg. Chem.* **1988**, *16*, 408–417. (b) Gellman, S. H.; Petter, R.; Breslow, R. *J. Am. Chem. Soc.* **1986**, *108*, 2388–2394.
- Clewly, R. G.; Slebocka-Jilk, H.; Brown, R. S. *Inorg. Chim. Acta* **1989**, *157*, 233–238.